

Thermal Decomposition of the Benzyl Radical to Fulvenallene (C_7H_6) + H

Gabriel da Silva,^{*,†} John A. Cole,[‡] and Joseph W. Bozzelli^{*,‡}

Department of Chemical and Biomolecular Engineering, The University of Melbourne, Victoria 3010, Australia, and Department of Chemistry and Environmental Science, New Jersey Institute of Technology, Newark, New Jersey 07102

Received: March 2, 2009; Revised Manuscript Received: April 1, 2009

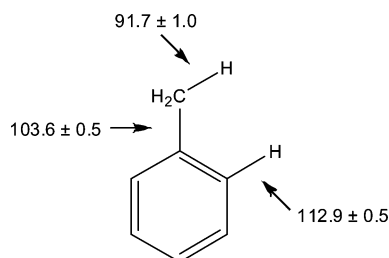
We show that the benzyl radical decomposes to the C_7H_6 fragment fulvenallene (+H), by first principles/RRKM study. Calculations using G3X heats of formation and B3LYP/6-31G(2df,p) structural and vibrational parameters reveal that the reaction proceeds predominantly via a cyclopentenyl-allene radical intermediate, with an overall activation enthalpy of ca. 85 kcal mol⁻¹. Elementary rate constants are evaluated using Eckart tunneling corrections, with variational transition state theory for barrierless C–H bond dissociation in the cyclopentenyl-allene radical. Apparent rate constants are obtained as a function of temperature and pressure from a time-dependent RRKM study of the multichannel multiwell reaction mechanism. At atmospheric pressure we calculate the decomposition rate constant to be $k [s^{-1}] = 5.93 \times 10^{35} T^{-6.099} \exp(-49\,180/T)$; this is in good agreement with experiment, supporting the assertion that fulvenallene is the C_7H_6 product of benzyl decomposition. The benzyl heat of formation is evaluated as 50.4 to 52.2 kcal mol⁻¹, using isodesmic work reactions with the G3X theoretical method. Some novel pathways are presented to the cyclopentadienyl radical (C_5H_5) + acetylene (C_2H_2), which may constitute a minor product channel in benzyl decomposition.

1. Introduction

The methylbenzenes, which include toluene, xylenes, and trimethylbenzenes, are of wide occurrence in combustion and atmospheric chemistry. These aromatic compounds are high-octane fuels, and their use in gasoline has increased since the phasing out of alkyllead octane boosters. Currently, the use of benzene in gasoline is also being reduced, as benzene is a suspected carcinogen. These two factors have led to an increase in the amount of alkylated benzenes present in gasoline, and a typical gasoline formulation may now contain around 15% toluene as well as significant amounts of xylene and other aromatics. In addition to their use in liquid fuels, substituted aromatics play important roles in benzene and soot formation, atmospheric chemistry, and the pyrolysis and oxidation of coal and biomass. As the parent (poly)alkylbenzene, much effort has been directed in the last 4–5 years toward better understanding the oxidation and pyrolysis of toluene and toluene fuel blends,^{1–19} but significant uncertainties still remain with respect to aspects of the kinetics and mechanism.

The resonantly stabilized benzyl radical is the major initial product in the oxidation of toluene. Bond dissociation energies (BDEs) for the benzyl–H, phenyl–CH₃ and methylphenyl–H bonds in toluene have been evaluated here, using the best available enthalpies of formation,^{20–25} and are illustrated in Scheme 1. There are three degenerate benzyl hydrogen atoms in toluene, and five phenyl hydrogen atoms (2 ortho, 2 meta, 1 para); the phenyl hydrogen atoms are assumed to be equivalent and are modeled using the benzene C–H BDE. Because of toluene's weak $C_6H_5CH_2-H$ bond, formation of the benzyl radical dominates over the phenyl and methylphenyl radicals at low temperatures, via respective unimolecular (dissociation) and bimolecular (abstraction) pathways. However, at even

SCHEME 1: Bond Dissociation Energies (kcal mol⁻¹) in Toluene^a



^a Calculated using experimental heats of formation (with uncertainties) from refs 20–25.

moderate combustion temperatures the higher-energy methylphenyl–H abstraction²⁶ and phenyl–CH₃ bond dissociation¹² reactions become important. The phenyl and methylphenyl radicals react rapidly with O₂, yielding species including the cyclopentadienyl radical, cyclopentadienone, the phenoxy radical (or their methyl substituted equivalents),^{2,27} and, in the case of *o*-methylphenyl radical oxidation, *o*-quinone methide.^{2,28} The benzyl + O₂ reaction is slow to produce new products, as the weak benzylperoxy adduct predominantly falls apart at relevant combustion conditions.²⁹ As a result, thermal decomposition of the benzyl radical, as well as bimolecular reactions with species such as OH and HO₂,³⁰ assume increased significance.

Due to its importance, benzyl decomposition has been studied extensively using a variety of experimental techniques. The products of benzyl decomposition, however, are unclear and have been the source of much debate. The kinetic data prior to 1992 has been critically evaluated by Baulch et al.,³¹ who suggest $k [s^{-1}] = 5.1 \times 10^{13} \exp(-36\,370/T)$ for the overall reaction of benzyl to $C_3H_3 + 2C_2H_2$, $C_4H_4 + C_3H_3$, $C_5H_5 + C_2H_2$, and C_7H_7 , in the temperature range 1350–1900 K. Branching ratios for these different product sets were not identified. A recent shock tube study on benzyl decomposition

* To whom correspondence should be addressed. E-mail: gdasilva@unimelb.edu.au (G.d.S.), bozzelli@njit.edu (J.W.B.).

[†] The University of Melbourne.

[‡] New Jersey Institute of Technology.

by Oehlschlaeger et al. at 1.5 bar and 1430–1730 K yielded k [s^{-1}] = $8.20 \times 10^{14} \exp(-40\,600/T)$,³² in good agreement with Baulch et al. The products, however, were assumed to be an unknown C_7H_6 fragment plus H. This assumption was based primarily on the results of Fröchtenicht et al.,³³ who used a molecular beam apparatus to photodissociate toluene and cycloheptatriene, producing activated benzyl radicals the decay of which was followed with mass spectrometry and observed to exclusively produce $C_7H_6 + H$. The formation of a C_7H_6 fragment in benzyl decomposition is also supported by the results of a recent atomic resonance absorption spectroscopy (ARAS) study,³⁴ which required one H atom to be produced per molecule of benzyl in order to accurately model toluene decomposition. A quantum chemical study on benzyl decomposition by Jones et al.³⁵ has suggested that $C_7H_6 + H$ could be formed by a ring-opening pathway to an open-chain C_7H_7 isomer, with an activation energy of around 97 kcal mol⁻¹. Dissociation of this radical to $CH_2CCHCHCHCCH$ ((Z)-1,2,4-heptatrien-6-yne) + H has been assumed to account for the unknown C_7H_6 fragment in benzyl decomposition,^{21,35} although this dissociation step would presumably require additional energy (when the activation energy for ring-opening is already considerably greater than that observed experimentally), while abstraction reactions from the open-chain radical would not account for the observation of free H atoms. Jones et al. additionally considered formation of $C_5H_5 + C_2H_2$ from the benzyl radical, via a 6-methylenebicyclo[3.1.0]hex-3-en-2-yl intermediate, and computed that this process would proceed at an almost identical rate to ring-opening. Seeing as the $C_7H_6 + H$ pathway is experimentally observed to dominate $C_5H_5 + C_2H_2$ formation and that the activation energy required for ring-opening followed by unimolecular dissociation to $C_7H_6 + H$ would be significantly greater than that observed experimentally for benzyl decomposition, a lower energy pathway to an unidentified C_7H_6 fragment must exist in the thermal decomposition of benzyl radicals.

It has recently been suggested that fulvenallene is the C_7H_6 product in benzyl decomposition.³⁶ Fulvenallene is not currently included in kinetic models of hydrocarbon combustion; however, small amounts of this C_7H_6 isomer have been detected in a lean gasoline flame containing ca. 4% C_7H_8 (presumably toluene) using photoionization mass spectrometry.³⁷ It is not entirely surprising that fulvenallene would be the major product of benzyl decomposition, considering that this species has been identified as the most stable isomer on the C_7H_6 potential energy surface.³⁸ Fulvenallene is also known as a product of phenylcarbene ring contraction,³⁹ and is produced (along with the benzyl radical) in the pyrolysis of benzylic compounds such as benzyl fluoride.⁴⁰ In the latter instance, it is unclear whether fulvenallene is partially formed from thermal decomposition of the benzyl radical or entirely via elimination of species such as HF to give phenylcarbene, which subsequently rearranges to fulvenallene.

Many comprehensive reaction mechanisms and kinetic models have been developed for the oxidation and pyrolysis of toluene, all of which prominently feature the benzyl radical.^{5,12,16–18,41–45} Unfortunately, the treatment of benzyl decomposition in these kinetic mechanisms is inconsistent (and in some cases completely absent) and does not consider pressure dependence. This is most likely due to the large number of studies on benzyl decomposition and uncertainty over the decomposition products and their rate of formation. For example, several kinetic models treat benzyl decomposition to the cyclopentadienyl radical +

C_2H_2 with an activation energy of only 70 kcal mol⁻¹ and to $C_4H_4 + C_3H_3$ with an activation energy of around 84 kcal mol⁻¹.

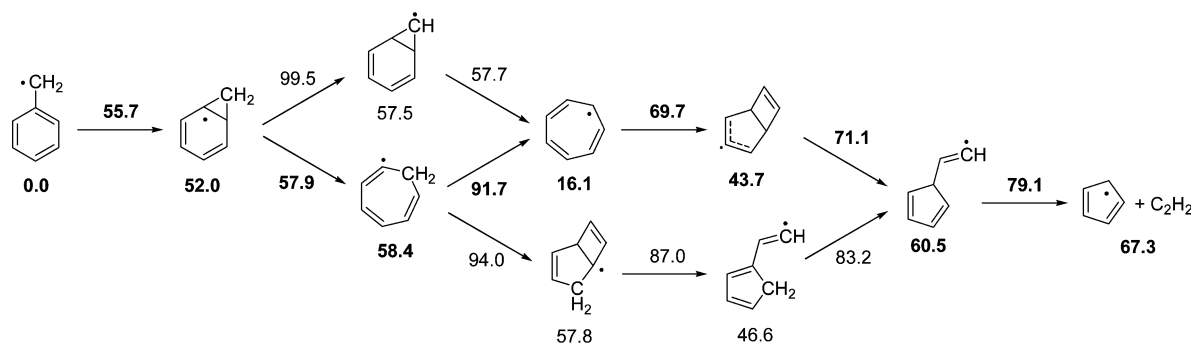
We have undertaken a first principles/RRKM study of benzyl decomposition to $C_7H_6 + H$. The findings of this study should lead to improved modeling of the combustion and atmospheric oxidation of substituted aromatics, soot formation, and also the pyrolysis of carbonaceous fuels like coal and biomass.

2. Computational Methods

Ab initio and density functional theory (DFT) calculations were performed using Gaussian 03.⁴⁶ Statistical mechanics and reaction rate theory calculations use ChemRate v. 1.5.2.⁴⁷ All species and transition states considered on the C_7H_7 potential energy surface are studied with the composite G3X theoretical method.⁴⁸ The G3X method utilizes B3LYP/6-31G(2df,p) geometries and frequencies, plus higher level energy corrections using HF through QCISD(T) theory with basis sets of decreasing size, along with empirical corrections for unpaired and valence electrons and spin-orbit coupling. The G3X method provides mean absolute deviations of 0.76 and 0.56 kcal mol⁻¹ for the respective radical and hydrocarbon subsets of the G3/99 test set and of 0.88 kcal mol⁻¹ across all enthalpies of formation.⁴⁸ The Gaussian-3 type methods also perform well for barrier heights and weakly bound complexes (somewhat representative of transition states). Using the BH6 test set of barrier heights, the related G3S method provides a mean unsigned error of 0.6 kcal mol⁻¹.⁴⁹ With the six hydrogen-bonded complexes of the G3/05 test set the G3X method yields a mean absolute deviation of 1.01 kcal mol⁻¹.⁵⁰ We conservatively estimate that our calculated barrier heights are accurate to ± 2 kcal mol⁻¹.

Standard enthalpies of formation ($\Delta_f H^\circ_{298}$) are obtained from atomization work reactions, using reference enthalpies (0 K) of 170.122 kcal mol⁻¹ for C⁵¹ and 51.634 kcal mol⁻¹ for H.²² Temperature-dependent thermochemistry is obtained from 300 to 3000 K using G3X standard enthalpies of formation and B3LYP/6-31G(2df,p) vibrational frequencies and moments of inertia. Low-frequency vibrational modes corresponding to internal rotation are treated as hindered rotors, from B3LYP/6-31G(d) rotor potentials. Corrections for molecular symmetry and optical isomers are applied where appropriate.

High-pressure limit rate constants (k^∞) for elementary reactions were calculated according to canonical transition state theory, from 300 to 3000 K. Relevant corrections for reaction degeneracy were incorporated in k^∞ . Calculated k^∞ values were fit to the modified Arrhenius equation $k^\infty = A'T^n \exp(-E_a/RT)$ to obtain the elementary rate parameters E_a (kcal mol⁻¹), A' (s⁻¹), and n , which we report here. Reactions involving an intramolecular hydrogen shift or C–H bond homolysis are corrected for tunneling of the H atom according to the Eckart theory.⁵² Here, the characteristic barrier length (l) is calculated from the transition state's imaginary frequency (ν_i) using eq 1.⁵³ In eq 1 E_1 and E_{-1} are the respective forward and reverse barrier heights at 0 K and μ is the reduced mass of H. Barrierless C–H dissociation in the cyclopentenyl-allene radical is treated using variational transition state theory.¹ The minimum energy potential for C–H bond dissociation was calculated at the UB3LYP/6-31G(2df,p) level of theory, scanning along the dissociating bond length in 0.1 Å intervals. The 0 K B3LYP energies were scaled by the 298 K G3X reaction enthalpy, providing accurate enthalpies of formation for discrete structures along the MEP. Frequency calculations were performed for each structure, confirming a single imaginary frequency with vibrational mode connecting the reactants and products. Temperature-dependent thermochemical properties and rate constants for each

SCHEME 2: Decomposition of the Benzyl Radical to Cyclopentadienyl (C₅H₅) + Acetylene (C₂H₂)^a

^a Enthalpies of reaction and activation (kcal mol⁻¹) calculated at the G3X level. Lowest energy pathway in bold.

structure on the MEP were calculated as described above, providing input for the variational analysis.

$$l = \sqrt{\frac{2(E_1^{-1/2} - E_{-1}^{-1/2})^{-2}}{\mu|v_1|^2}} \quad (1)$$

It is difficult to assess the uncertainty in our rate constant calculations. Similar rate constant treatment to that employed here (G3-RAD structures and energies, Eckart tunneling, free rotor model) for the benzene + methyl radical abstraction reaction was found to reproduce experimental rate constants to within a factor of ca. 1.0–1.2.⁵⁴ We estimate that our rate constant calculations are accurate to around a factor of 2 in the pre-exponential factor ($A'T'$), with a 2 kcal mol⁻¹ uncertainty in E_a .

Apparent, or observed, rate constants for decomposition of the benzyl radical are calculated as a function of temperature (300–3000 K) and pressure (0.001–1000 atm), using RRKM theory with a time-dependent solution of the master equation. Collisional energy transfer is treated using an exponential down model with $\langle\Delta E_{\text{down}}\rangle = 2000 \text{ cm}^{-1}$ (vide infra). Collision parameters for benzyl (and other C₇H₇ isomers) are assumed to be the same as those for toluene. Argon is used as the bath gas.

3. Results and Discussion

3.1. Reaction Mechanism. Cyclopentadienyl (C₅H₅) + Acetylene (C₂H₂). As noted in the Introduction, recent results indicate that a C₇H₆ species is the main decomposition product of the benzyl radical. However, theoretical and experimental studies have often considered the products C₅H₅ + C₂H₂. While this study is concerned principally with the formation of C₇H₆, we also present some preliminary results on benzyl dissociation to C₅H₅ + C₂H₂. A reaction mechanism for C₅H₅ + C₂H₂ formation is depicted in Scheme 2, featuring G3X reaction and activation enthalpies. Several of the pathways here are known in the literature,^{35,55} although some novel reactions are also presented. The lowest-energy reaction pathway (in bold) requires a maximum reaction barrier of 91.7 kcal mol⁻¹; this is 6.8 kcal mol⁻¹ higher in energy than the mechanism we present for fulvenallene + H production (vide infra) but may still provide a significant contribution to the overall benzyl decomposition rate. Further calculations are required to evaluate the importance of this novel mechanism. Kinetics of the reverse C₅H₅ + C₂H₂ association reaction, which is important in soot formation,⁵⁵ should also be evaluated.

(Z)-1,2,4-Heptatrien-6-yne + H. The first C₇H₆ mechanism in benzyl decomposition that we consider is the ring-opening pathway. Figure 1 shows an energy diagram for ring-opening of the benzyl radical, followed by dissociation of the weak C–H

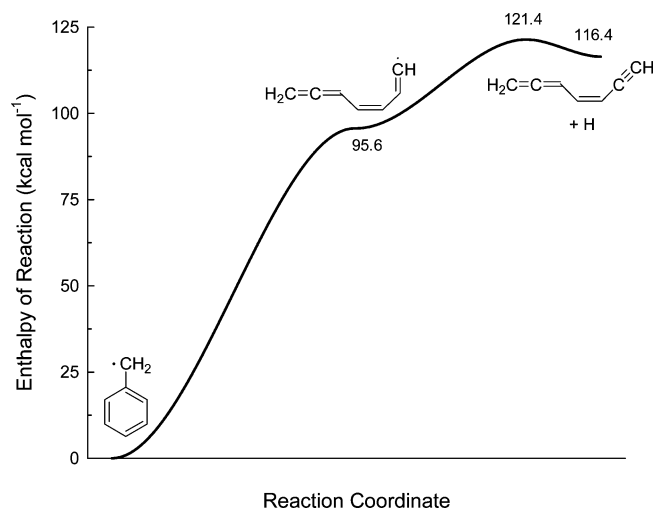
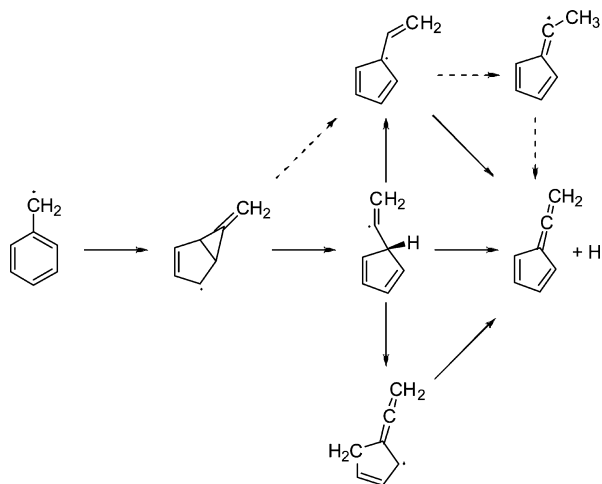


Figure 1. Decomposition of the benzyl radical to (Z)-1,2,4-heptatrien-6-yne + H, via a ring-opening pathway.

bond to yield the C₇H₆ isomer (Z)-1,2,4-heptatrien-6-yne. The minimum energy pathway is constructed in Figure 1 and in later energy diagrams using the theory of harmonic parabolic wells.⁵⁶ The initial ring-opening reaction step is barrierless at the G3X level, with a reaction enthalpy of 95.6 kcal mol⁻¹. This is already significantly higher than the experimentally measured activation energy (e.g., 72.3 or 80.7 kcal mol⁻¹), but might be offset by the high pre-exponential factor for this essentially barrierless C–C bond dissociation reaction. However, following ring-opening, the C–H bond dissociation step to (Z)-1,2,4-heptatrien-6-yne + H presents a further barrier of 25.8 kcal mol⁻¹, giving a total barrier height of 121.4 kcal mol⁻¹. We therefore consider this reaction pathway to be unimportant and do not investigate it further.

Fulvenallene + H. We consider decomposition of the benzyl radical to the C₇H₆ species fulvenallene + H. Our calculations reveal that fulvenallene can form via C–H bond dissociation in the four C₇H₇ isomers depicted in Scheme 3. However, only three of these pathways are energetically competitive and are investigated here.⁵⁷ Energy diagrams for these three pathways, based on 298 K enthalpies of formation, are presented in Figures 2–4. Similar reaction schemes have also been proposed by Cavallotti et al.^{36a}

Figures 2–4 show that benzyl decomposition is initiated by contraction of the C₆ ring to form a bicyclic species (2), which subsequently ring opens to a cyclopentadiene-ethenyl radical (3). This second step requires the greater overall barrier, with a transition state that is 70.3 kcal mol⁻¹ above the benzyl radical. Following ring-opening, 3 can lose the weak H atom on the cyclopentadiene ring, yielding fulvenallene (4) + H (Figure 2).

SCHEME 3: Reaction Pathways for the Formation of Fulvenallene + H in the Thermal Decomposition of the Benzyl Radical^a


^a Dashed arrows indicate high-energy pathways that are not considered further.

The transition state for this dissociation step is loose and falls 88.3 kcal mol⁻¹ above the benzyl radical. Alternatively, **3** can undergo an intramolecular hydrogen shift to either the cyclopentadienyl-ethene radical (**5**) as in Figure 3 or the cyclopentenyl-allene radical (**6**) as in Figure 4. Species **5** is formed with a barrier 88.2 kcal mol⁻¹ above the benzyl radical and subsequently dissociates to fulvenallene + H in a lower-energy near-barrierless reaction. This pathway may therefore be competitive with that depicted in Figure 2. Formation of **6** proceeds at 76.4 kcal mol⁻¹ above the benzyl radical and dissociates to fulvenallene + H in a barrierless reaction. The total barrier for the reaction pathway depicted in Figure 4 is therefore only 84.9 kcal mol⁻¹, making this the most energetically favorable decomposition mechanism (in the work of Cavallotti et al.,^{36a} the total barrier height for this pathway is reported as 81.6 kcal mol⁻¹, with a discrete transition state structure lying slightly above fulvenallene + H in energy). The barrierless C–H dissociation step is also entropically favored, reflected in the large pre-exponential factor for this reaction (vide infra). Jones et al.³⁵ showed that C–H bond dissociation in the cyclopentadiene-ethenyl radical (**3**) can also lead to formation of the C₇H₆ isomer 5-ethynyl-1,3-cyclopentadiene, with a barrier 99 kcal mol⁻¹ above benzyl. Figures 2–4 reveal that decomposition of the benzyl radical to fulvenallene + H proceeds with lower barriers than any other previously considered pathways.

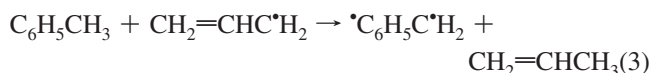
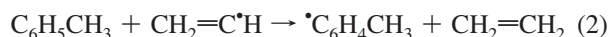
Dissociation of the cyclopentadiene-ethenyl radical (**3**) to the alternate C₇H₆ product 5-ethynyl-1,3-cyclopentadiene (plus H) was considered by Jones et al.³⁵ and they found that this decomposition pathway proceeded with an overall activation energy 99.0 kcal mol⁻¹ above that of benzyl. We have also studied this reaction process, and at the G3X level we obtain a heat of formation of 94.51 kcal mol⁻¹ for 5-ethynyl-1,3-cyclopentadiene, and 147.75 kcal mol⁻¹ for the C–H dissociation transition state; this yields an overall enthalpy of activation of 95.39 kcal mol⁻¹ and reaction enthalpy of 94.25 kcal mol⁻¹. Comparatively, dissociation of the weaker C–H bond in **3** to fulvenallene + H requires 88.3 kcal mol⁻¹, while the lower energy pathway depicted in Figure 4 requires only 84.9 kcal mol⁻¹. We therefore conclude that the formation of 5-ethynyl-1,3-cyclopentadiene + H will be negligible relative to fulvenallene + H in the thermal decomposition of benzyl.

An alternative mechanism for benzyl decomposition is proposed by Braun-Unkoff et al.,²¹ where benzyl is assumed to isomerize to another C₇H₇ species (suggested to be either a ring-opening or ring compound) with k [s⁻¹] = $3.16 \times 10^{15} \exp(-85\,200/RT)$. It was then suggested that this isomer dissociates to a C₇H₆ species + H with an activation energy of 36.8 kcal mol⁻¹. The energy diagram provided in Figure 1 suggests that this C₇H₆ molecule is not (*Z*)-1,2,4-heptatrien-6-yne, because of the large barrier for initial ring-opening and negligible barrier for reverse reaction to benzyl. It is possible that the intermediate C₇H₇ isomer is the cyclopentadienyl-ethene (**5**) and/or cyclopentenyl-allene (**6**) radical, which are formed with barriers of around 80 to 90 kcal mol⁻¹ and subsequently dissociate to fulvenallene + H with relatively low barriers and large pre-exponential factors. However, further kinetic modeling will be required to validate or discard this proposed mechanism. We note that the Braun-Unkoff rate expression derived for benzyl isomerization is in close agreement with the rate expression for benzyl decomposition of Oehlschlaeger et al.³²

3.2. Thermochemistry. Thermochemical properties have been calculated for all minima and transition states in the proposed benzyl decomposition mechanisms. Enthalpies of formation ($\Delta_f H^\circ_{298}$) obtained at the G3X level from atomization enthalpies are listed in Table 1. Entropies (S°_{298}) and heat capacities [$C_p(T)$, 300–3000 K] are available in the Supporting Information, along with geometries, vibrational frequencies, and moments of inertia.

From Table 1 we find that the enthalpy of formation of benzyl is 52.37 kcal mol⁻¹ at the G3X level of theory. There have been numerous prior experimental measurements of this property, although significant uncertainties remain. While there are several earlier determinations of $\Delta_f H^\circ_{298}$ in the range of around 49–50 kcal mol⁻¹,^{58,59} a recent analysis of the literature¹⁰ recommends a value of 51.5 ± 1.0 kcal mol⁻¹.²¹ This latter result is within error of our calculated heat of formation for the benzyl radical. Following benzyl, the second most stable C₇H₇ isomer studied here is the cyclopentadiene-ethene radical (**5**), with $\Delta_f H^\circ_{298} = 72.40$ kcal mol⁻¹. This species is ca. 20 kcal mol⁻¹ less stable than the benzyl radical, making it comparable in energy to the methylphenyl radicals (2-methylphenyl $\Delta_f H^\circ_{298} = 74.5 \pm 2$ kcal mol⁻¹).² The relatively high degree of stability of this species results from an allylic radical structure. Fulvenallene, where $\Delta_f H^\circ_{298} = 85.20$ kcal mol⁻¹, is seen to be almost 20–30 kcal mol⁻¹ more stable than singlet phenylcarbene,^{60,61} a common C₇H₆ isomer. While we are unaware of any prior experimental or ab initio determinations of the fulvenallene heat of formation, it has been previously estimated as 82 kcal mol⁻¹ using group additivity,⁶¹ in relative agreement with the present result.

Isodesmic reactions have been used to further investigate the benzyl radical heat of formation. The higher-energy phenyl C–H bond dissociations in toluene, leading to the *o*-, *m*-, and *p*-methylphenyl radicals, have also been studied. Isodesmic reactions feature the same number and type of bonds on either side of the reaction and result in significant improvements in calculated BDEs and heats of formation through cancelation of systematic errors.⁶² We have calculated C–H BDEs in toluene using the following work reactions:



In eq 2, the phenyl C–H bonds in toluene are modeled using the ethene C–H bond; it is well-known that bonds on phenyl

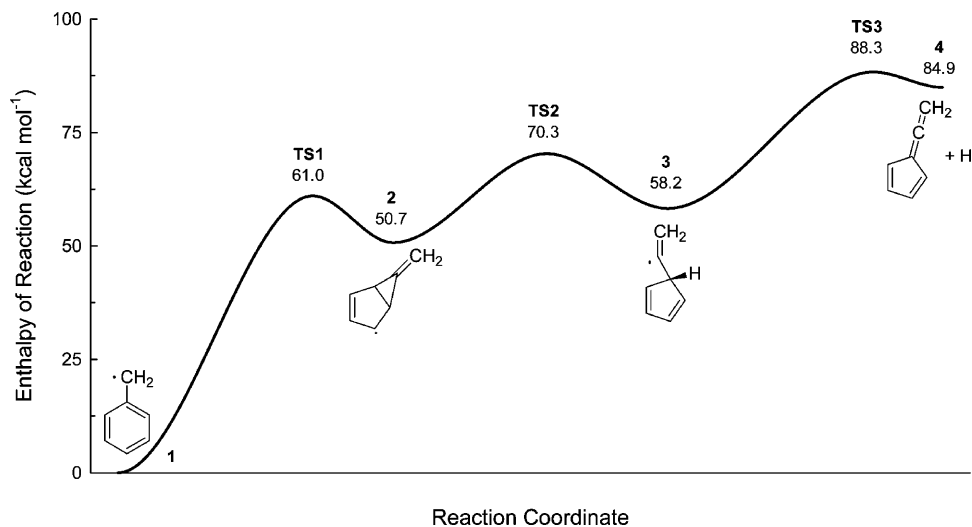


Figure 2. Decomposition of the benzyl radical to fulvenallene + H from cyclopentadiene-ethenyl radical (3). Dissociation of 3 to 5-ethynyl-1,3-cyclopentadiene + H occurs via a transition state with a heat of formation of 147.75 kcal mol⁻¹.

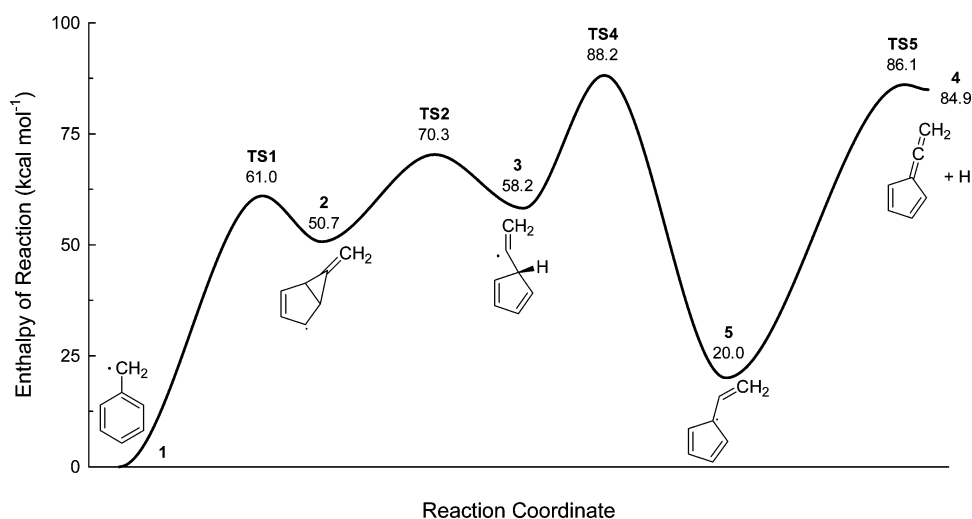


Figure 3. Decomposition of the benzyl radical to fulvenallene + H from cyclopentadienyl-ethene radical (5).

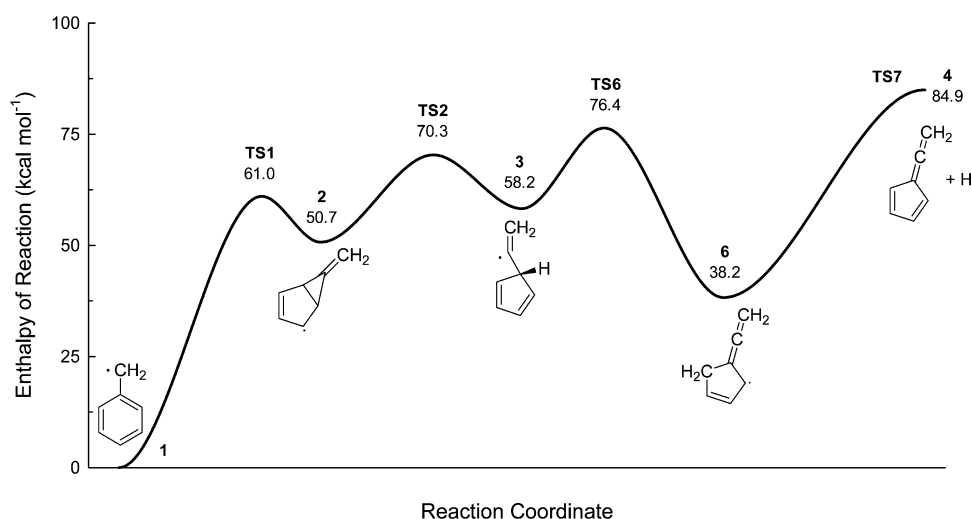


Figure 4. Decomposition of the benzyl radical to fulvenallene + H from cyclopentenyl-allene radical (6).

and vinyl sites are similar in energy, with the phenyl bonds typically being around 3 kcal mol⁻¹ stronger.⁶³ The benzyl C–H bond in toluene is modeled in eq 3 using the similar allylic C–H BDE in propene. Experimental values of 110.7 ± 0.6 and 88.8 ± 0.4 kcal mol⁻¹ have been used for the relevant BDEs in

ethene and propene.⁶⁴ Calculated isodesmic BDEs are listed in Table 2, along with heats of formation for the C₇H₇ radicals (calculated using Δ_fH^o₂₉₈ = 11.95 kcal mol⁻¹ for toluene).²⁰ Included in Table 2 are radical enthalpies calculated using atomization work reactions and BDEs derived from these

TABLE 1: Standard Enthalpies of Formation ($\Delta_f H^\circ_{298}$, kcal mol⁻¹) for Minima and Transition States in the Benzyl \rightarrow Fulvenallene + H Mechanism, from G3X Calculations^a

	$\Delta_f H^\circ_{298}$ (kcal mol ⁻¹)
1	52.37
2	103.07
3	110.62
4	85.20
5	72.40
6	90.62
TS1	113.39
TS2	122.70
TS3	140.69
TS4	140.55
TS5	138.46
TS6	128.75

^a Species defined in Figures 2–4.**TABLE 2: Bond Dissociation Energies (BDEs) and Radical Heats of Formation ($\Delta_f H^\circ_{298}$) for C–H Dissociation in Toluene from Isodesmic and Atomization G3X Calculations^a**

R' (toluene \rightarrow R' + H)	isodesmic		atomization	
	BDE	$\Delta_f H^\circ_{298}$ (R')	BDE	$\Delta_f H^\circ_{298}$ (R')
benzyl	92.4	52.2	91.2	52.4
<i>o</i> -methylphenyl	114.8	74.7	114.1	75.4
<i>m</i> -methylphenyl	114.8	74.7	114.1	75.3
<i>p</i> -methylphenyl	115.4	75.3	114.7	75.9

^a All values in kcal mol⁻¹.

enthalpies using an atomization heat of formation for toluene (13.32 kcal mol⁻¹). The isodesmic and atomization calculations both return a similar heat of formation for benzyl, being 52.2 and 52.4 kcal mol⁻¹, respectively. However, if an alternate value of 87.0 ± 1.0 kcal mol⁻¹ is used for the allylic propene BDE,⁶⁵ then the isodesmic benzyl heat of formation is 50.4 kcal mol⁻¹. The isodesmic BDE is over 1 kcal mol⁻¹ greater than the atomization value, where the atomization result is in better agreement with the bulk of the experimental data. This is a result of the considerable difference between the experimental and atomization heats of formation of toluene (11.95 and 13.32 kcal mol⁻¹, respectively). For the methylphenyl radicals we obtain heats of formation of around 75 kcal mol⁻¹ with both the isodesmic and atomization calculations. Isodesmic BDEs are calculated to be around 115 kcal mol⁻¹, while atomization BDEs are around 114 kcal mol⁻¹. These BDEs are somewhat greater than the suggested experimental value (112.9 kcal mol⁻¹), although there is some support in the literature for a benzene C–H bond energy on the order of 114 to 115 kcal mol⁻¹. The three methylphenyl radical isomers are all similar in energy, with the para isomer being less stable than the others by 0.6 kcal mol⁻¹.

3.3. Transition State Geometries and Elementary Rate Parameters. Transition state structures have been located for each elementary reaction and are depicted here in Figure 5. Dissociation of **6** to fulvenallene + H via **TS7** proceeds without any intrinsic barrier (i.e., barrierless association reaction) and therefore does not demonstrate a discrete transition state structure. Instead, this reaction has been treated using variational transition state theory (see below). High-pressure rate parameters E_a , A' , and n for all elementary reactions involved in the decomposition of benzyl to fulvenallene + H are listed in Table 3. Bimolecular fulvenallene + H rate constants (in units of cm³ mol⁻¹ s⁻¹) are included, but are not required to model benzyl decomposition.

The rate constant for barrierless dissociation of the cyclopentenyl-allene radical (**6**) to fulvenallene + H has been calculated with variational transition state theory, following the general procedure of da Silva and Bozzelli.¹ The minimum energy pathway (MEP) for C–H bond dissociation has been calculated at the B3LYP/6-31G(2df,p) level and scaled by the G3X reaction enthalpy (46.68 kcal mol⁻¹) (Figure 6). Rate constants have been evaluated at discrete points along the MEP and minimized to obtain the variational rate constant. Rate constants for the forward and reverse reactions, from 300 to 3000 K, have been fit to the three-parameter Arrhenius equation. For the forward dissociation reaction we obtain k^∞ [s⁻¹] = $1.02 \times 10^{13} T^{0.342} \exp(-23\,500/T)$, and for the reverse association reaction we find k^∞ [cm³ mol⁻¹ s⁻¹] = $1.27 \times 10^{11} T^{0.854} \exp(-145/T)$.

The variational transition state for C–H bond scission in the cyclopentenyl-allene radical (**TS7**) is located at a C–H bond length of 2.10 Å from 300 to 600 K, 2.00 Å from 700 to 1500 K, and 1.90 Å from 1600 to 3000 K. This is similar to the C–H bond length in **TS5** (2.16 Å, cf. Figure 5), which is actually a more endothermic reaction but exhibits a discrete transition state because of the large structural rearrangement from an allylic-type radical to the allene geometry. By comparison, **TS7** requires little structural change. For C–H bond dissociation in the cyclopentadienyl-ethene radical (**TS3**) we find a somewhat tighter transition state structure (1.89 Å), along with the largest barrier (above the dissociated products) for any of these dissociation reactions. This is a result of both significant structural change and the relatively small reaction enthalpy (ca. 27 kcal mol⁻¹).

3.4. Decomposition Kinetics. Apparent rate constants for decomposition of the benzyl radical to fulvenallene + H have been calculated from RRKM theory with master equation analysis for falloff, for $P = 0.001$ –1000 atm and $T = 300$ –3000 K. The three decomposition mechanisms depicted in Figures 2–4 result in a multiwell multichannel reaction system. Simulations were performed with the three contributing transition state geometries for C–H dissociation in the cyclopentenyl-allene radical (**TS7**), locating the transition state in $k(E)$ according to microcanonical variational transition state theory. The minimum rate constant for this reaction channel resulted from the 2.10 Å transition state for 300–400 K, the 2.00 Å transition state for 500–1500 K, and the 1.90 Å transition state for 2000–3000 K. Apparent rate constants for benzyl decomposition are listed in Table 4 as a function of pressure, in the form $k = A' T^n \exp(-E_a/RT)$. Rate constants represent the total reaction rate, i.e., the sum of the three reaction channels. Across the entire pressure range the activation energy (E_a) is around 90–100 kcal mol⁻¹. The value of n , which is a measure of nonlinearity in an Arrhenius inverse log plot, is seen to steadily increase in magnitude with decreasing pressure, as a result of falloff. Approaching the high-pressure limit, the pre-exponential factor ($A = A' T^n$) is around 10^{16} s⁻¹.

Branching ratios for the three reaction channels leading to fulvenallene + H are plotted in Figure 7, at 1 atm pressure. Not surprisingly, decomposition proceeds predominantly via barrierless C–H dissociation in the cyclopentenyl-allene radical at most temperatures considered. At low (<700 K) and high (>2500 K) temperatures decomposition via H loss from the cyclopentadienyl-ethenyl radical becomes dominant. At lower temperatures this is due to stabilization of the cyclopentenyl-allene radical, where the barriers for forward and reverse reaction are both relatively large. This is of little consequence, however, because the rate of decomposition at such low temperatures is almost negligible. At higher temperatures, the cyclopentadiene-

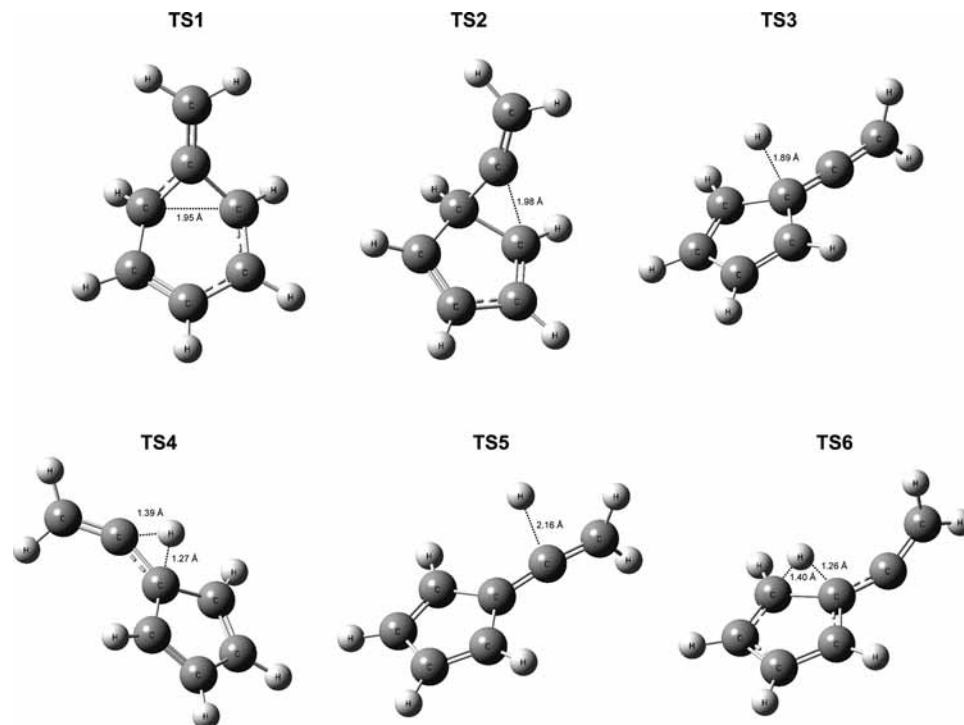


Figure 5. Transition state geometries in the benzyl decomposition mechanism. Calculated at the B3LYP/6-31G(2df,p) level of theory.

TABLE 3: Elementary Rate Parameters (E_a , A' , and n) for Forward and Reverse Reactions in the Benzyl Decomposition Mechanism^a

	forward			reverse		
	E_a	A'	n	E_a	A'	n
1 → 2 [TS1]	61.54	6.68×10^{12}	0.426	10.95	5.64×10^{12}	0.159
2 → 3 [TS2]	20.26	3.26×10^{13}	0.128	12.33	1.24×10^{11}	0.580
3 → 4 + H [TS3]	29.58	3.94×10^8	1.566	3.16	2.97×10^8	1.612
3 → 5 [TS4]	25.00	3.32×10^3	2.752	63.52	2.05×10^5	2.371
5 → 4 + H [TS5]	66.17	1.24×10^{11}	1.086	1.23	3.03×10^9	1.513
3 → 6 [TS6]	16.71	4.84×10^8	1.265	37.00	2.46×10^{10}	0.816
6 → 4 + H [TS7] ^b	46.70	1.02×10^{13}	0.342	-0.073	1.27×10^{11}	0.854

^a High-pressure-limit rate constants, $k^\infty = A'T^n \exp(-E_a/RT)$. Units: k^∞ and A' in s^{-1} or $\text{cm}^3 \text{mol}^{-1} \text{s}^{-1}$, E_a in kcal mol^{-1} , and T in K. ^b From variational transition state theory.

ethenyl mechanism becomes dominant due to the larger pre-exponential factor for dissociation of this radical to fulvenallene + H, compared to the lower-energy isomerization to the cyclopentenyl-allene radical. At all temperatures, decomposition via the cyclopentadienyl-ethene radical is relatively unimportant (less than 10%), as the formation of this species proceeds with both a large barrier and a small pre-exponential factor.

Figure 8 shows a 3D plot of the total rate constant for benzyl decomposition to fulvenallene + H, as a function of temperature and pressure. At 1000 atm we approach the high-pressure limit for temperatures up to around 2000 K. For lower pressures, falloff begins to become important for typical combustion/pyrolysis temperatures (ca. 1000–2000 K).

To provide a comparison to the experimental data at typical pyrolysis temperatures, two-parameter Arrhenius fits [$k = A \exp(-E_a/RT)$] have been obtained for 1000–2000 K from plots of $\ln k$ vs $1/T$ (Table 5). At lower pressures, these inverse log plots yield relatively poor linear relationships, due to the high degree of falloff at 2000 K. Good linear relationships were found for 1 atm and above ($R^2 > 0.997$). For these higher pressures E_a is in the range of 79–84 kcal mol^{-1} , with A being around 10^{14} – 10^{15} s^{-1} . These values compare well with the experimental results of ref 32, where $E_a = 80.67 \text{ kcal mol}^{-1}$ and $A = 8.2 \times$

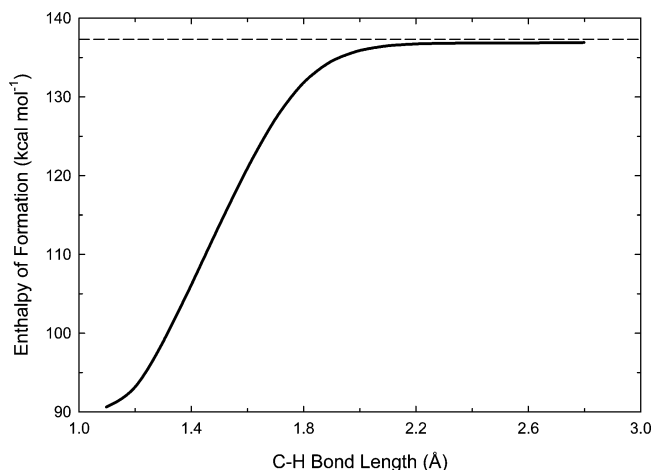


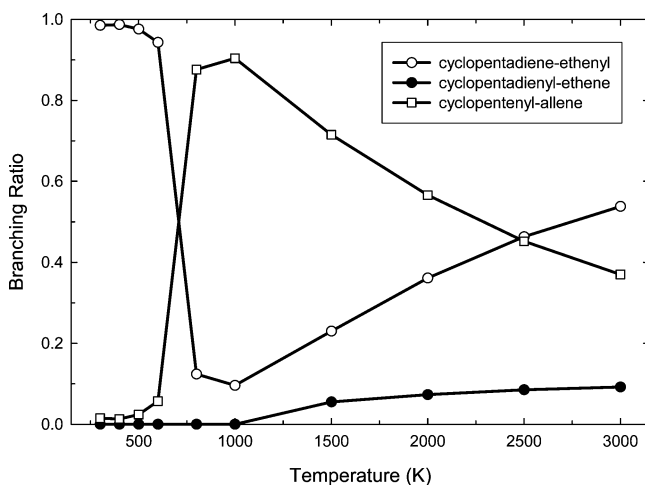
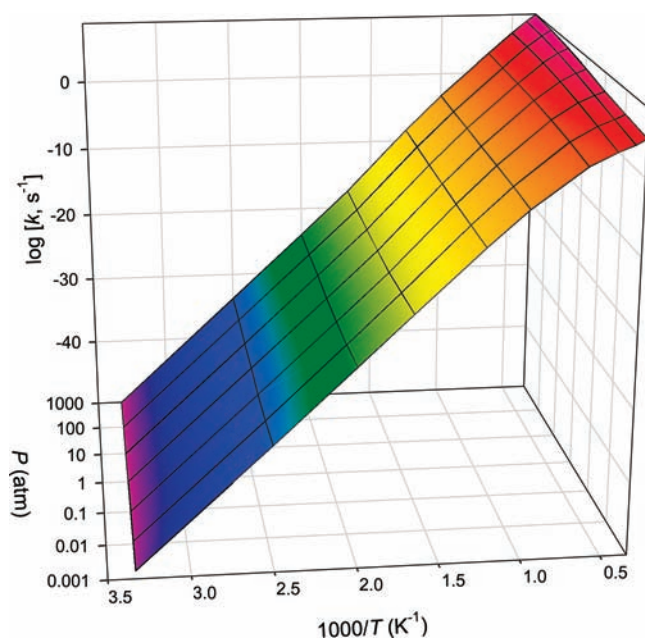
Figure 6. Minimum energy pathway for C–H bond dissociation in the cyclopentenyl-allene radical (6). Enthalpy values from B3LYP/6-31G(2df,p) energies, scaled by the G3X reaction enthalpy. Dashed line indicates $\Delta_f H_{298}^\circ$ of separated products (fulvenallene + H, 137.30 kcal mol^{-1}).

10^{14} s^{-1} . The rate constant recommendations of ref 31 give a lower (i.e., faster) activation energy (66.90 kcal mol^{-1}) but also a smaller (i.e., slower) value of A ($5.1 \times 10^{13} \text{ s}^{-1}$).

TABLE 4: Apparent Rate Parameters for Decomposition of Benzyl to Fulvenallene + H, as a Function of Pressure, from RRKM Analysis

P (atm)	E_a (kcal mol ⁻¹)	A' (s ⁻¹)	n
1×10^{-3}	101.40	2.15×10^{55}	-12.377
1×10^{-2}	101.54	1.67×10^{50}	-10.654
1×10^{-1}	99.97	1.25×10^{43}	-8.394
1×10^0	97.72	5.93×10^{35}	-6.099
1×10^1	95.85	1.04×10^{30}	-4.297
1×10^2	94.32	3.06×10^{25}	-2.890
1×10^3	93.40	6.28×10^{22}	-2.056

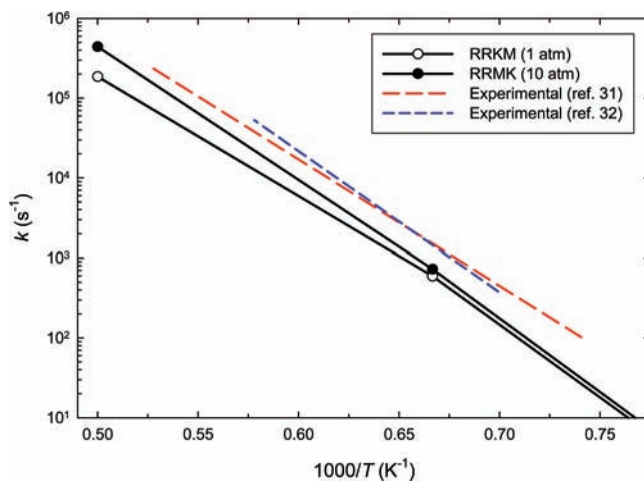
Figure 9 compares our fitted rate constants from 1000 to 2000 K (with $P = 1$ and 10 atm) to the experimental results of Baulch et al.³¹ and Oehlschlaeger et al.³² The measurements of ref 32 are for ca. 1.5 bar pressure, while the recommendations of the Baulch et al. review are based principally on experimental results at 2 bar. From Figure 9 there is seen to be good agreement

**Figure 7.** Branching ratios for the cyclopentadiene-ethenyl, cyclopentadienyl-ethene, and cyclopentenyl-allene reaction channels (Figures 2, 3, and 4, respectively) in the fulvenallene + H decomposition mechanism, at 1 atm.**Figure 8.** Calculated total rate constant (k , s⁻¹) for decomposition of benzyl to fulvenallene + H, as a function of temperature and pressure.**TABLE 5: Apparent Activation Energies (E_a) and Pre-Exponential Factors (A) for Decomposition of Benzyl to Fulvenallene + H from 1000 to 2000 K, as a Function of Pressure, from RRKM Analysis**

P (atm)	E_a (kcal mol ⁻¹)	A (s ⁻¹)
1×10^{-3}	63.08	2.74×10^{10}
1×10^{-2}	68.91	6.75×10^{11}
1×10^{-1}	74.50	1.20×10^{13}
1×10^0	79.07	1.16×10^{14}
1×10^1	82.13	5.06×10^{14}
1×10^2	83.87	1.09×10^{15}
1×10^3	84.05	1.26×10^{15}

between the calculated rate constants and both sets of experimental data, certainly to within the combined error of experiment and theory (see Supporting Information). Agreement between our calculations and both sets of experimental data is relatively good across the entire temperature range, with the calculated rate constants being low by less than an order of magnitude at 1 atm (and even less at 10 atm). The good accord between theory and experiment suggests that fulvenallene is the unidentified C₇H₆ fragment in benzyl decomposition.

We now examine the effect of $\langle \Delta E_{\text{down}} \rangle$ on the decomposition kinetics of the benzyl radical. RRKM calculations were performed using $\langle \Delta E_{\text{down}} \rangle$ values of 500 and 2000 cm⁻¹, at a pressure of 1.5 bar and from 1300 to 2000 K (in 100 K intervals). These temperature and pressure conditions were chosen to be representative of those used in the experiments of Oehlschlaeger et al., as well as the experimental data used in the critical evaluation of Baulch et al. Figure 10 shows a comparison of these calculated and experimental rate constants for benzyl decomposition. We find that a $\langle \Delta E_{\text{down}} \rangle$ value on the order of 2000 cm⁻¹ is required to accurately reproduce the experimental falloff behavior at higher temperatures. For lower values of $\langle \Delta E_{\text{down}} \rangle$ there is relatively good agreement between theory and experiment at around 1400 K and below but significant discrepancies at greater temperatures due to falloff effects. For the higher values of $\langle \Delta E_{\text{down}} \rangle$ there is good agreement between our calculations and both sets of experimental data across the entire experimental temperature range. Fitting the 2000 cm⁻¹ results to a two-parameter Arrhenius equation, and using our estimated uncertainties, we obtain an activation energy of 74.5 ± 2.0 kcal mol⁻¹ and an A factor of 4.0×10^{13} s⁻¹ (where $\log A = 13.60 \pm 0.30$). Comparatively,

**Figure 9.** Comparison between theoretical ($P = 1, 10$ atm) and experimental rate constants for thermal decomposition of the benzyl radical.

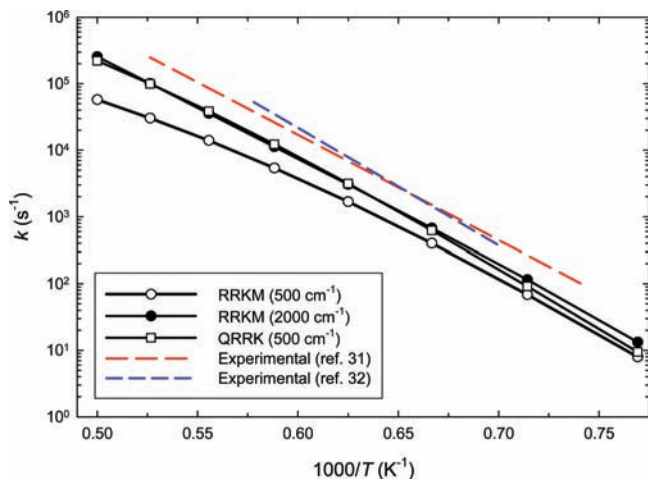


Figure 10. Comparison between theoretical (RRKM and QRRK) and experimental rate constants for thermal decomposition of the benzyl radical.

Baulch et al. recommend very similar values of $E_a = 72.27$ kcal mol⁻¹ and $A = 5.1 \times 10^{13}$ s⁻¹. Agreement is also very good with the data of Oehlschlaeger et al. ($E_a = 80.67$ kcal mol⁻¹ and $A = 8.2 \times 10^{14}$ s⁻¹), especially at lower temperatures, although their larger activation energy results in some divergence at higher temperatures. In the Supporting Information we demonstrate that agreement between our results and those of Baulch et al. is well within the combined uncertainty of the theoretical and experimental results. Close agreement between theory and experiment can be achieved when the barrier for decomposition is reduced by around 1 kcal mol⁻¹, which would imply a fulvenallene heat of formation that is closer to 84 kcal mol⁻¹ (given that the controlling step proceeds with only a thermodynamic barrier); further work is required to refine the thermochemistry of this new combustion intermediate.

In addition to the RRKM calculations, a quantum Rice–Ramsperger–Kassel (QRRK) calculation using $\langle \Delta E_{\text{down}} \rangle = 500$ cm⁻¹ and a master equation model for collisional energy transfer has been performed,^{66–68} and the results are included in Figure 10. The QRRK and RRKM calculations demonstrate excellent agreement for temperatures up to around 1500 K. At higher temperatures, the 500 cm⁻¹ RRKM results experience greater falloff than the corresponding QRRK results, which are now in close agreement with the 2000 cm⁻¹ RRKM rate constants. While the values of $\langle \Delta E_{\text{down}} \rangle$ required to reproduce falloff using RRKM theory at around 1600 K and above are large, they reflect similar results from a recent study of pyrazole decomposition,⁶⁹ and are not unexpected in the context of a temperature-dependent energy transfer model. Similar agreement with experiment is obtained using a reasonable temperature-dependent $\langle \Delta E_{\text{down}} \rangle$ value of $1 \times T$ cm⁻¹. One explanation for the large values of $\langle \Delta E_{\text{down}} \rangle$ required in our simulations is that in the shock tube experiments toluene and its products are playing a role in collisional energy transfer. The effect of this would be to increase the apparent value of $\langle \Delta E_{\text{down}} \rangle$ in our simulations, with toluene being a significantly better collider than argon. Further experimental results across a broader temperature and pressure range are required in order to better probe falloff effects and collisional energy transfer in the benzyl decomposition system.

Comparing the fulvenallene + H pathway to either C₅H₅ + C₂H₂ formation or to the C₇H₇ ring-opening mechanism (even neglecting further dissociation to (Z)-1,2,4-heptatrien-6-yne + H) indicates that both these paths should be relatively unimportant. Dissociation of benzyl isomers to other C₇H₆ products

like 5-ethenyl-1,3-cyclopentadiene, which are presently believed to all be higher in energy, should also be insignificant. We therefore conclude that fulvenallene is the previously unidentified C₇H₆ product in benzyl decomposition and that fulvenallene + H are the primary decomposition products of the benzyl radical. Of course, fulvenallene can undergo further pyrolysis and oxidation reactions, possibly providing some of the species previously proposed as benzyl decomposition products. For instance, fulvenallene could decompose to a C₃H₂ species plus C₄H₄ (or 2C₂H₂), followed by abstraction or dissociation reactions to C₃H₃. The further reactions of fulvenallene, which are currently unknown, will need to be included in detailed kinetic models of aromatic combustion.

Finally, it will also be of interest to consider the thermal decomposition of substituted benzyl radicals. For example, in the decomposition of 2,6-substituted benzyl radicals (like the 2,6-dichloro-1-benzyl radical) the reaction mechanism depicted in Figure 4 is now unavailable. However, the secondary mechanism of Figure 2 may be more rapid than in benzyl decomposition, through weakening of the dissociating C–X bond in the cyclopentadiene-ethenyl radical. Such effects will need to be considered in the oxidation kinetics of polysubstituted aromatics.

Acknowledgment. This research was partially supported by the U.S. Air Force Phase II STTR (contract number FA8650-06-C-2658).

Supporting Information Available: Molecular geometries (Cartesian coordinates); G3X energies (hartrees), vibrational frequencies, and moments of inertia for all minima and transition states; entropy (S°_{298}) and heat capacity [$C_p(T)$] values; internal rotor potential in **3**; and comparison of experimental and theoretical rate expressions, with associated uncertainties. This material is available free of charge via the Internet at <http://pubs.acs.org>.

Note Added in Proof. Since submitting this article a recent photoionization mass spectrometry study of a toluene flame has come to our attention,⁷⁰ in which high levels of fulvenallene are detected. The peak fulvenallene mole fraction is 53% that of benzyl, with both occurring at the same distance from the burner (temperature). This new result strongly supports our assertion that fulvenallene is the major decomposition product of benzyl.

References and Notes

- da Silva, G.; Bozzelli, J. W. *J. Phys. Chem. A* **2008**, *112*, 3566.
- da Silva, G.; Chen, C.-C.; Bozzelli, J. W. *J. Phys. Chem. A* **2007**, *111*, 8663.
- Mittal, G.; Sung, C.-J. *Combust. Flame* **2007**, *150*, 355.
- Oehlschlaeger, M. A.; Davidson, D. F.; Hanson, R. K. *Proc. Combust. Inst.* **2007**, *31*, 211.
- Andrae, J.; Björnbom, P.; Cracknell, R. F.; Kalghatgi, G. *Combust. Flame* **2007**, *149*, 2.
- Hermans, I.; Peeters, J.; Vereecken, L.; Jacobs, P. A. *ChemPhysChem* **2007**, *8*, 2678.
- Yahyaoui, M.; Djebaïli-Chaumeix, N.; Dagaut, P.; Paillard, C.-E.; Heyberger, B.; Pengloan, G. *Int. J. Chem. Kinet.* **2007**, *39*, 518.
- Herzler, J.; Fikri, M.; Hitzbleck, K.; Starke, R.; Schulz, C.; Roth, P.; Kalghatgi, G. T. *Combust. Flame* **2007**, *149*, 25.
- Sivaramakrishnan, R.; Tranter, R. S.; Brezinsky, K. *J. Phys. Chem. A* **2006**, *110*, 9388.
- Sivaramakrishnan, R.; Tranter, R. S.; Brezinsky, K. *J. Phys. Chem. A* **2006**, *110*, 9400.
- Pritchard, H. O. *Phys. Chem. Chem. Phys.* **2006**, *8*, 4559.
- Oehlschlaeger, M. A.; Davidson, D. F.; Hanson, R. K. *Combust. Flame* **2006**, *147*, 195.

- (13) Andrae, J.; Johansson, D.; Björnbohm, P.; Risberg, P.; Kalghatgi, G. *Combust. Flame* **2005**, *140*, 267.
- (14) Vasudevan, V.; Davidson, D. F.; Hanson, R. K. *J. Phys. Chem. A* **2005**, *109*, 3352.
- (15) Hoorn, J. A. A.; Alsters, P. L.; Versteeg, G. F. *Int. J. Chem. Reactor Eng.* **2005**, *3*, A6.
- (16) Sivaramakrishnan, R.; Tranter, R. S.; Brezinsky, K. *Proc. Combust. Inst.* **2005**, *30*, 1165.
- (17) Bounaceur, R.; Da Costa, I.; Fournet, R.; Billaud, F.; Battin-Leclerc, F. *Int. J. Chem. Kinet.* **2005**, *37*, 25.
- (18) Sivaramakrishnan, R.; Tranter, R. S.; Brezinsky, K. *Combust. Flame* **2004**, *139*, 340.
- (19) Gauthier, B. M.; Davidson, D. F.; Hanson, R. K. *Combust. Flame* **2004**, *139*, 300.
- (20) Prosen, E. J.; Gilmont, R.; Rossini, F. D. *J. Res. NBS* **1945**, *34*, 65; toluene $\Delta_f H^\circ_{298} = 11.95 \pm 0.15$ kcal mol⁻¹.
- (21) Braun-Unkthoff, M.; Frank, P.; Just, T. *Ber. Bunsen-Ges. Phys. Chem.* **1990**, *94*, 1417; benzyl $\Delta_f H^\circ_{298} = 51.5 \pm 1.0$ kcal mol⁻¹.
- (22) Chase, M. W., Jr. *J. Phys. Chem. Ref. Data, Monogr.* **1998**, *1*; H $\Delta_f H^\circ_{298} = 52.103 \pm 0.001$ kcal mol⁻¹.
- (23) Ruscic, B.; Litorja, M.; Asher, R. L. *J. Phys. Chem. A* **1999**, *103*, 8625; CH₃ $\Delta_f H^\circ_{298} = 35.05 \pm 0.07$ kcal mol⁻¹.
- (24) Cioslowski, J.; Schimeczek, M.; Liu, G.; Stoyanov, V. *J. Chem. Phys.* **2000**, *113*, 9377; benzene $\Delta_f H^\circ_{298} = 19.7 \pm 0.2$ kcal mol⁻¹.
- (25) Ervin, K. M.; DeTuri, V. F. *J. Phys. Chem. A* **2002**, *106*, 9947; phenyl $\Delta_f H^\circ_{298} = 80.5 \pm 0.5$ kcal mol⁻¹.
- (26) Uc, V. H.; Alvarez-Idaboy, J. R.; Galano, A.; García-Cruz, I.; Vivier-Bunge, A. *J. Phys. Chem. A* **2006**, *110*, 10155.
- (27) (a) Tokmakov, I. V.; Kim, G.-S.; Kislov, V. V.; Mebel, A. M.; Lin, M. C. *J. Phys. Chem. A* **2005**, *109*, 6114. (b) Fadden, M. J.; Barckholtz, C.; Hadad, C. M. *J. Phys. Chem. A* **2000**, *104*, 3004. (c) Barckholtz, C.; Fadden, M. J.; Hadad, C. M. *J. Phys. Chem. A* **1999**, *103*, 8108. (d) Mebel, A. M.; Lin, M. C. *J. Am. Chem. Soc.* **1994**, *116*, 9577. (e) Yu, T.; Lin, M. C. *J. Am. Chem. Soc.* **1994**, *116*, 9571. (f) Carpenter, B. K. *J. Am. Chem. Soc.* **1993**, *115*, 9806.
- (28) da Silva, G.; Bozzelli, J. W. *J. Phys. Chem. A* **2007**, *111*, 7987.
- (29) Murakami, Y.; Oguchi, T.; Hashimoto, K.; Nosaka, Y. *J. Phys. Chem. A* **2007**, *111*, 13200.
- (30) da Silva, G.; Bozzelli, J. W. *Proc. Combust. Inst.* **2009**, *32*, 287.
- (31) Baulch, D. L.; Cobos, C. J.; Cox, R. A.; Esser, C.; Frank, P.; Just, T.; Kerr, J. A.; Pilling, M. J.; Troe, J.; Walker, R. W.; Warnatz, J. *J. Phys. Chem. Ref. Data* **1992**, *21*, 411.
- (32) Oehlschlaeger, M. A.; Davidson, D. F.; Hanson, R. K. *J. Phys. Chem. A* **2006**, *110*, 6649.
- (33) Fröchtenicht, R.; Hippler, H.; Troe, J.; Toennies, J. P. *J. Photochem. Photobiol. A: Chem.* **1994**, *80*, 33.
- (34) Eng, R. A.; Gebert, A.; Goos, E.; Hippler, H.; Kachiani, C. *Phys. Chem. Chem. Phys.* **2002**, *4*, 3989.
- (35) Jones, J.; Bacskey, G. B.; Mackie, J. C. *J. Phys. Chem. A* **1997**, *101*, 7105.
- (36) (a) Cavallotti, C.; Derudi, M.; Rota, R. *Proc. Combust. Inst.* **2009**, *32*, 115. (b) da Silva, G.; Bozzelli, J. W. 20th International Symposium on Gas Kinetics; Manchester UK, 20–25 July 2008; P49. (c) da Silva, G.; Bozzelli, J. W. Chemeca 2008; Newcastle, Australia, 28 September–1 October 2008; 103.
- (37) Huang, C.; Wei, L.; Yang, B.; Wang, J.; Sheng, L.; Zhang, Y.; Qi, F. *Energy Fuels* **2006**, *20*, 1505.
- (38) Wong, M. W.; Wentrup, C. *J. Org. Chem.* **1996**, *61*, 7022.
- (39) Crow, W. D.; Paddon-Row, M. N. *J. Am. Chem. Soc.* **1972**, *94*, 4746.
- (40) Schissel, P.; Kent, M. E.; McAdoo, D. J.; Hedaya, E. *J. Am. Chem. Soc.* **1970**, *92*, 2147.
- (41) Pitz, W. J.; Seiser, R.; Bozzelli, J. W.; Seshadri, K.; Chen, C.-J.; Da Costa, I.; Fournet, R.; Billaud, F.; Battin-Leclerc, F.; Westbrook, C. K. Chemical Kinetic Study of Toluene Oxidation under Premixed and Nonpremixed Conditions. Report UCRL-CONF-201575; Lawrence Livermore National Laboratory: Livermore, CA, 2003.
- (42) Dagaut, P.; Pengloan, G.; Ristori, A. *Phys. Chem. Chem. Phys.* **2002**, *4*, 1846.
- (43) Alexiou, A.; Williams, A. *Combust. Flame* **1996**, *104*, 51.
- (44) Colket, M. B.; Seery, D. *J. Proc. Combust. Inst.* **1994**, *25*, 883.
- (45) Emdee, J. L.; Brezinsky, K.; Glassman, I. *J. Phys. Chem.* **1992**, *96*, 2151.
- (46) Frisch, M. J.; Trucks, G. W.; Schlegel, H. B.; Scuseria, G. E.; Robb, M. A.; Cheeseman, J. R.; Montgomery, J. A., Jr.; Vreven, T.; Kudin, K. N.; Burant, J. C.; Millam, J. M.; Iyengar, S. S.; Tomasi, J.; Barone, V.; Mennucci, B.; Cossi, M.; Scalmani, G.; Rega, N.; Petersson, G. A.; Nakatsuji, H.; Hada, M.; Ehara, M.; Toyota, K.; Fukuda, R.; Hasegawa, J.; Ishida, M.; Nakajima, T.; Honda, Y.; Kitao, O.; Nakai, H.; Klene, M.; Li, X.; Knox, J. E.; Hratchian, H. P.; Cross, J. B.; Adamo, C.; Jaramillo, J.; Gomperts, R.; Stratmann, R. E.; Yazyev, O.; Austin, A. J.; Cammi, R.; Pomelli, C.; Ochterski, J. W.; Ayala, P. Y.; Morokuma, K.; Voth, G. A.; Salvador, P.; Dannenberg, J. J.; Zakrzewski, V. G.; Dapprich, S.; Daniels, A. D.; Strain, M. C.; Farkas, O.; Malick, D. K.; Rabuck, A. D.; Raghavachari, K.; Foresman, J. B.; Ortiz, J. V.; Cui, Q.; Baboul, A. G.; Clifford, S.; Cioslowski, J.; Stefanov, B. B.; Liu, G.; Liashenko, A.; Piskorz, P.; Komaromi, I.; Martin, R. L.; Fox, D. J.; Keith, T.; Al-Laham, M. A.; Peng, C. Y.; Nanayakkara, A.; Challacombe, M.; Gill, P. M. W.; Johnson, B.; Chen, W.; Wong, M. W.; Gonzalez, C.; Pople, J. A. *Gaussian 03, Revision D.01*; Gaussian, Inc.: Wallingford, CT, 2004.
- (47) Mokrushin, V.; Bedanov, V.; Tsang, W.; Zachariah, M.; Knyazev, V. *ChemRate, Version 1.5.2*; National Institute of Standards and Testing: Gaithersburg, MD, 2006.
- (48) Curtiss, L. A.; Redfern, P. C.; Raghavachari, K.; Pople, J. A. *J. Chem. Phys.* **2001**, *114*, 108.
- (49) Lynch, B. J.; Truhlar, D. G. *J. Phys. Chem. A* **2003**, *107*, 8996.
- (50) Curtiss, L. A.; Redfern, P. C.; Raghavachari, K. *J. Chem. Phys.* **2005**, *123*, 124107.
- (51) Ruscic, B.; Pinzon, R. E.; Morton, M. L.; von Laszewski, G.; Bittner, S. J.; Nijssure, S. G.; Amin, K. A.; Minkoff, M.; Wagner, A. F. *J. Phys. Chem. A* **2004**, *108*, 9979.
- (52) Eckart, C. *Phys. Rev.* **1930**, *35*, 1303.
- (53) Tokmakov, I. V.; Park, J.; Gheysas, S.; Lin, M. C. *J. Phys. Chem. A* **1999**, *103*, 3636.
- (54) Hemelsoet, K.; Moran, D.; Van Speybroeck, V.; Waroquier, M.; Radom, L. *J. Phys. Chem. A* **2006**, *110*, 8942.
- (55) Fascella, S.; Cavallotti, C.; Rota, R.; Carrà, S. *J. Phys. Chem. A* **2005**, *109*, 7546.
- (56) da Silva, G.; Kennedy, E. M.; Dlugogorski, B. Z. *J. Phys. Org. Chem.* **2007**, *20*, 167.
- (57) Direct formation of **5** from **2** exhibits a barrier height of 130.3 kcal mol⁻¹. Isomerization of **5** to the C₅H₄=C[•]CH₃ radical requires a barrier of 93.0 kcal mol⁻¹.
- (58) Ruscic, B.; Boggs, J. E.; Burcat, A.; Csazar, A. G.; Demaison, J.; Janoschek, R.; Martin, J. M. L.; Morton, M.; Rossi, M. J.; Stanton, J. F.; Szalay, P. G.; Westmoreland, P. R.; Zabel, F.; Berces, T. *J. Phys. Chem. Ref. Data* **2005**, *34*, 573.
- (59) Hippler, H.; Troe, J. *J. Phys. Chem.* **1990**, *94*, 3803.
- (60) Nguyen, T. L.; Kim, G.-S.; Mebel, A. M.; Nguyen, M. T. *Chem. Phys. Lett.* **2001**, *349*, 571.
- (61) Poutsma, J. C.; Nash, J. J.; Paulino, J. A.; Squires, R. R. *J. Am. Chem. Soc.* **1997**, *119*, 4686.
- (62) (a) Raghavachari, K.; Stefanov, B. B.; Curtiss, L. A. *J. Chem. Phys.* **1997**, *106*, 6764. (b) da Silva, G.; Bozzelli, J. W. *J. Chem. Phys. A* **2006**, *110*, 12977. (c) da Silva, G.; Sebban, N.; Bozzelli, J. W.; Bockhorn, H. *ChemPhysChem* **2006**, *7*, 1119.
- (63) (a) da Silva, G.; Kim, C.-H.; Bozzelli, J. W. *J. Phys. Chem. A* **2006**, *110*, 7925. (b) da Silva, G.; Chen, C.-C.; Bozzelli, J. W. *Chem. Phys. Lett.* **2006**, *424*, 42.
- (64) Blanksby, S. J.; Ellison, G. B. *Acc. Chem. Res.* **2003**, *36*, 255.
- (65) Seetula, J. A. *Phys. Chem. Chem. Phys.* **1999**, *1*, 4727.
- (66) Chang, A. Y.; Bozzelli, J. W.; Dean, A. M. *Z. Phys. Chem.* **2000**, *214*, 1533.
- (67) Sheng, C. Y.; Bozzelli, J. W.; Dean, A. M.; Chang, A. Y. *J. Phys. Chem. A* **2002**, *106*, 7276.
- (68) Bozzelli, J. W.; Chang, A. Y.; Dean, A. M. *Int. J. Chem. Kinet.* **1997**, *29*, 161.
- (69) da Silva, G. *Chem. Phys. Lett.* **2009**, doi: 10.1016/j.cplett.2009.04.011.
- (70) Li, Y.; Zhang, L.; Tian, Z.; Yuan, T.; Wang, J.; Yang, B.; Qi, F. *Energy & Fuels* **2009**, *23*, 1473–1485.